

Title	Synchrotron radiation-based Mössbauer spectra of ^{174}Yb measured with internal conversion electrons
Author(s)	Masuda, Ryo; Kobayashi, Yasuhiro; Kitao, Shinji; Kurokuzu, Masayuki; Saito, Makina; Yoda, Yoshitaka; Mitsui, Takaya; Iga, Fumitoshi; Seto, Makoto
Citation	Applied Physics Letters (2014), 104(8)
Issue Date	2014-02
URL	http://hdl.handle.net/2433/184915
Right	© 2014 AIP Publishing LLC
Type	Journal Article
Textversion	publisher



Synchrotron radiation-based Mössbauer spectra of ^{174}Yb measured with internal conversion electrons

Ryo Masuda, Yasuhiro Kobayashi, Shinji Kitao, Masayuki Kurokuzu, Makina Saito, Yoshitaka Yoda, Takaya Mitsui, Fumitoshi Iga, and Makoto Seto

Citation: *Applied Physics Letters* **104**, 082411 (2014); doi: 10.1063/1.4866280

View online: <http://dx.doi.org/10.1063/1.4866280>

View Table of Contents: <http://scitation.aip.org/content/aip/journal/apl/104/8?ver=pdfcov>

Published by the [AIP Publishing](#)

NEW
Model PS-100
Preconfigured Tabletop
Probe Station



*An affordable solution for
a wide range of research*

The advertisement features a photograph of the Model PS-100 probe station, a complex piece of scientific equipment with various mechanical components and a probe. The background is a gradient of blue and white.

Synchrotron radiation-based Mössbauer spectra of ^{174}Yb measured with internal conversion electrons

Ryo Masuda,^{1,a)} Yasuhiro Kobayashi,¹ Shinji Kitao,¹ Masayuki Kurokuzu,¹ Makina Saito,² Yoshitaka Yoda,³ Takaya Mitsui,⁴ Fumitoshi Iga,⁵ and Makoto Seto^{1,4}

¹Research Reactor Institute, Kyoto University, Kumatori-cho, Sennan-gun, Osaka 590-0494, Japan

²Beamline Spectroscopy/Scattering Group, Elettra-Sincrotrone Trieste, S. S. 14 Km 163.5, I-34149 Trieste, Italy

³Research and Utilization Division, Japan Synchrotron Radiation Research Institute, Kouto, Sayo-cho, Sayo-gun, Hyogo 679-5198, Japan

⁴Condensed Matter Science Division, Japan Atomic Energy Agency, Kouto, Sayo-cho, Sayo-gun, Hyogo 679-5148, Japan

⁵College of Science, Ibaraki University, Mito, Ibaraki, 310-8512, Japan

(Received 16 December 2013; accepted 6 February 2014; published online 27 February 2014)

A detection system for synchrotron-radiation (SR)-based Mössbauer spectroscopy was developed to enhance the nuclear resonant scattering counting rate and thus increase the available nuclides. In the system, a windowless avalanche photodiode (APD) detector was combined with a vacuum cryostat to detect the internal conversion (IC) electrons and fluorescent X-rays accompanied by nuclear de-excitation. As a feasibility study, the SR-based Mössbauer spectrum using the 76.5 keV level of ^{174}Yb was observed without ^{174}Yb enrichment of the samples. The counting rate was five times higher than that of our previous system, and the spectrum was obtained within 10 h. This result shows that nuclear resonance events can be more efficiently detected by counting IC electrons for nuclides with high IC coefficients. Furthermore, the windowless detection system enables us to place the sample closer to the APD elements and is advantageous for nuclear resonant inelastic scattering measurements. Therefore, this detection system can not only increase the number of nuclides accessible in SR-based Mössbauer spectroscopy but also allows the nuclear resonant inelastic scattering measurements of small single crystals or enzymes with dilute probe nuclides that are difficult to measure with the previous detection system. © 2014 AIP Publishing LLC. [<http://dx.doi.org/10.1063/1.4866280>]

Mössbauer spectroscopy is a well-established method with applications in various fields, including physics, chemistry, biology, and earth science. It provides element-specific information on the probe nuclide's electronic states, including valence and magnetism, even in complex materials. With regard to the probe nuclide, the Mössbauer effect has been observed in approximately 100 nuclides of nearly 50 elements, and Mössbauer spectroscopy with these nuclides is expected. However, Mössbauer studies have been performed mostly using ^{57}Fe , ^{119}Sn , and ^{151}Eu . One major difficulty in Mössbauer spectroscopy using other nuclides is preparation and storage of radioactive isotopes (RI) as γ -ray sources. Some RI sources have short lifetimes and are unsuitable for use in Mössbauer measurements over long times. Some RI sources are formed by nuclear reactions that require an accelerator. These difficulties are notably alleviated by using synchrotron radiation (SR) as the Mössbauer spectroscopy source. SR has broad spectra, and we can extract X-rays with the required energy (usually <100 keV). Additionally, SR has far higher brilliance than γ -rays from RI, and thus electronic states can be studied under extreme conditions, e.g., high pressure. Therefore, nuclear resonant scattering (NRS) experiments using various nuclides of various materials have been performed using SR. In NRS of SR experiments, the most frequently used method has been nuclear forward scattering (NFS) spectroscopy.¹ This method enables efficient

measurements in the time region, and hyperfine interactions can be elucidated from the quantum beat pattern of the decay spectra. In these experiments, avalanche photodiode (APD) detectors are usually used to detect scattered X-rays because of their high time resolution and tolerance to high counting rates. However, APD detection efficiency decreases as the X-ray energy increases and thus NRS of SR by nuclides with high nuclear resonance energy required improvements. This means that if the detection efficiency for NRS of SR is improved, then the nuclides available for Mössbauer spectroscopy using SR are extended.^{2,3} In 2009, an energy-domain method was reported, and ^{73}Ge SR-based Mössbauer spectroscopy using its 68.8 keV level was performed in 90 h as a feasibility study.⁴ This method allows us to see the Mössbauer spectra in the energy region. Analysis of the complex samples seems to be easier than the NFS method because the spectrum obtained is similar to that of conventional Mössbauer spectroscopy using RI sources, for which there is a large amount of accumulated knowledge.⁵⁻⁷ This method also improves the detection efficiency of NRS of SR by detecting fluorescent X-rays that follow the internal conversion (IC) process along with the direct nuclear-resonant-scattered X-rays. The fluorescent X-rays have lower energies than the direct X-rays and are easier to detect. Additionally, the IC coefficient, which is the ratio of the IC process to the direct nuclear-resonant-scattered X-ray process, is higher than 1 in many nuclides; thus, the fluorescent X-ray intensity is stronger than that of the direct X-rays in

^{a)}Electronic mail: masudar@rii.kyoto-u.ac.jp

NRS of SR by these nuclides. Along with the fluorescent X-rays, electrons, called IC electrons, are also emitted in the IC process. Therefore, the detection of IC electrons added to the fluorescent X-rays and the direct scattered X-rays appears to be a very promising way to enhance detection efficiency because the IC electron detection efficiency is usually higher than that of the X-rays. For example, the detection efficiency of electrons below 100 keV by an APD with a 150 μm depletion layer is almost 100% while the efficiency of even 30 keV X-rays is about 4%. The detection of IC electrons is well known in conventional RI Mössbauer spectroscopy as conversion electron Mössbauer spectroscopy,⁸ and IC electrons have already been measured in NRS of SR by ^{197}Au .⁹ However, in previous NRS spectroscopies, the APD detectors usually used beryllium X-ray windows for protection from visible light, which also block the electrons scattered from samples. Therefore, we developed a detection system, comprising an X-ray-windowless APD detector and a sample chamber with a He-flow cryostat. Along with its ability to detect the electrons, the windowless detection system makes it possible to place the sample closer to the APD elements. An increase in the solid angle covered by the APD further enhances the counting rate. As a feasibility study, this system was applied to ^{174}Yb SR-based Mössbauer spectroscopy. ^{174}Yb is the most abundant Yb nuclide (natural abundance of 31.8%) but is not the most frequently used nuclide for Yb Mössbauer spectroscopy. Obviously, investigation of the Yb electronic states is important to understand the various magnetic properties caused by its $4f$ electrons, and Mössbauer spectroscopy has mainly been performed using ^{170}Yb to study valence and magnetism properties.⁶ Although the natural abundance of ^{170}Yb is only 3%, it is the most popular nuclide in Mössbauer spectroscopy because γ -ray source preparation for ^{170}Yb is easier than that for ^{174}Yb . The γ -ray source for ^{174}Yb was made through a ^{176}Yb ($p, 3n$) ^{174}Lu reaction and requires an accelerator¹⁰ while that for ^{170}Yb can be prepared by neutron irradiation of ^{169}Tm , which has natural abundance of 100%. However, because RI source preparation difficulties do not apply when SR is the light source, we can select a well-conditioned nuclide for SR-based Mössbauer spectroscopy. In fact, nuclear resonant excitation of the 76.5 keV level of ^{174}Yb by SR has already been observed by detecting the fluorescent X-rays.¹¹ Here, we report on instrumentation for SR-based Mössbauer spectroscopy using the developed system and the SR-based ^{174}Yb Mössbauer spectrum as a feasibility study.

The experimental setup for SR-based Mössbauer spectroscopy is shown in Fig. 1. The experiments were

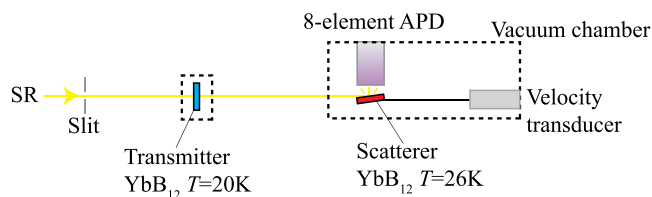


FIG. 1. Schematic drawing of the experimental set-up for the ^{174}Yb Mössbauer spectrum of YbB_{12} . The line with the arrow indicates the SR path. The rectangle with dashed lines shows the vacuum region. The APD detector and scatterer were in the same vacuum chamber for IC electron detection.

performed at the BL09XU and BL11XU undulator beamlines of SPring-8. The electron-storage ring's operating mode was the "203 bunch" mode with an electron-bunch interval of 23.6 ns. The SR was monochromatized to approximately 5 eV around the ^{174}Yb nuclear resonance by using a Si (333) monochromator and then transmitted a sample in a cryostat (the "transmitter" in Fig. 1). Downstream of the transmitter, the SR was scattered by a sample in another cryostat (the "scatterer" in Fig. 1). The scatterer in this cryostat can be moved using a velocity transducer to measure the Mössbauer spectrum at low temperatures. The scatterer's temperature was monitored at its holder by a silicon diode thermometer. The emission from the scatterer was detected using a developed detector with an eight-element APD for the IC electrons placed above the scatterer in the cryostat. The distance between the scatterer and the APD was approximately 5 mm, and the detector was insulated in heat against the scatterer by vacuum. The detection area of each element was $3 \times 5 \text{ mm}^2$, and the depletion layer of each element was 150 μm thick. Almost all of the elements' surfaces were uncovered apart from the limited area required for the Au electrical contact. Because NRS by ^{174}Yb is emitted with a delay (76.5 keV level half-life $t_{1/2} = 1.79 \text{ ns}$), NRS was counted in the time window between 6.1 ns and 13.6 ns after SR incidence. The NRS before 6.1 ns could not be counted because of the tremendous and prompt electronic scattering (ES). Using this set-up, we performed two experiments: First, to verify the electron detection, we compared the intensity from the scatterer with and without an electron shield placed between scatterer and APD detector; second, we measured an actual Mössbauer spectrum. In the first experiment, the shield was a 17 μm -thick Al foil. The transmitter was not used in this case, and the scatterer was a 7 mm-diameter pellet of YbAl_2 powder with thickness of 158 mg/cm^2 YbAl_2 ; the measurements were performed at room temperature in a 0.04 Pa vacuum to collect the IC electrons. In the second experiment, the sample situations were quite different. Both transmitter and scatterer were YbB_{12} powdered from a single crystal.¹² The reason why YbB_{12} is used for our Mössbauer measurement is its high recoilless fraction, which affects the absorption depth of the spectrum. Both YbB_{12} powders were mixed with boron nitride and made into 7 mm-diameter pellets. The transmitter thickness was 60.9 mg/cm^2 YbB_{12} while that of the scatterer was 736 mg/cm^2 YbB_{12} . The transmitter was set at 20 K in a $<0.01 \text{ Pa}$ vacuum, and the scatterer was set at 26 K in a $<0.01 \text{ Pa}$ vacuum. All samples were used without ^{174}Yb enrichment.

In the first experiment, the delayed NRS counting rates were 2.3 counts per second (cps) with Al foil and 17.2 cps without the foil. Those of the ES were 1.0×10^7 cps with the foil and 3.0×10^7 cps without the foil. For the ES, the main process is the photoelectric process, through which photoelectrons and fluorescent X-rays are emitted. Here, the main component of the photoelectric process is from the electron K-shell and the cross section is approximately six times higher than the sum of the cross sections of the L-shells, which are the second main component. However, the kinetic energy of each photoelectron from the K-shell is only 15 keV and they cannot travel more than 1.4 μm

(0.9 mg/cm^2) in YbAl_2 . In contrast, the energy of the photoelectrons from the L-shells is approximately 66 keV, and they can travel up to $16 \mu\text{m}$ (10 mg/cm^2) in YbAl_2 . Therefore, compared with the photoelectrons from the L-shells, those from the K-shell suffer severe losses due to self-absorption by the scatterer. Thus, the main component of the detected electrons was photoelectrons from the L-shells while that of the detected X-rays was fluorescent K X-rays. Because the transmission rate of fluorescent K X-rays is >0.99 through the $17 \mu\text{m}$ Al foil, while many of the L-shell photoelectrons are stopped by the foil, the strong reduction of ES with the foil demonstrates the APD's ability to detect the emitted electrons. For the NRS, the ratio of the counting rate without the foil to that with the foil is much higher than that in ES. This is because of the difference between the NRS process and the ES process; the branching ratio to the L-edge is more than three times higher than that to the K-edge in the IC process, and the IC process through the electron L-edge is the most frequently occurring of these processes in NRS.¹³ Therefore, the emitted X-rays in NRS were mainly fluorescent L X-rays, which have lower energy than K X-rays and were not counted in our measurement because their signal levels were lower than the discriminator circuit threshold limit. Consequently, the main component of the detected photons in the NRS was the weaker fluorescent K X-rays through the IC process, while that of the detected electrons was IC electrons from the L-shells. In this way, the ratio of detected electrons to detected X-rays in the NRS was much higher than the ratio in the ES and confirmed that the windows shielding for electrons affect the NRS detection. Therefore, the effectiveness of IC electron detection in NRS of SR by ^{174}Yb was demonstrated.

The ^{174}Yb Mössbauer spectrum observed over 10 hours in the second experiment is shown in Fig. 2. The NRS counting rate was 6 cps, while that of ES was 1.5×10^7 cps. In our previous ^{174}Yb SR-based Mössbauer spectroscopy trial using an eight-element APD with an X-ray window, the ES rate was 1.0×10^7 cps and that of NRS was 1.2 cps. Therefore, the actual counting rates were five times higher than those measured using the previous method. The spectrum was evaluated using the formulae in Refs. 4 and 14. From these formulae, the evaluated isomer shift is $-0.05 \pm 0.05 \text{ mm/s}$, i.e. no shifts were observed; this is expected, because the transmitter and the scatterer were formed from the same

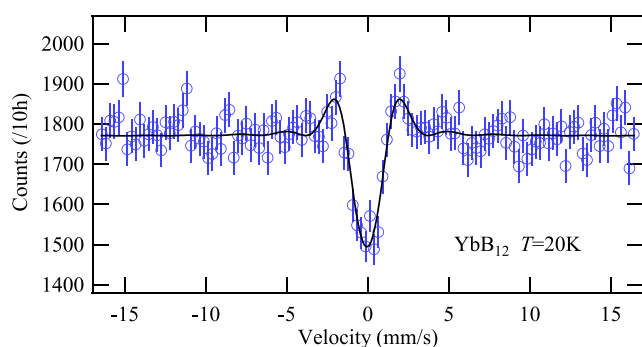


FIG. 2. ^{174}Yb Mössbauer spectrum of YbB_{12} . The transmitter was YbB_{12} at 20 K, and the scatterer was YbB_{12} at 26 K. The circles are the experimental data, and the error bars are attached to the data circles. The curved line indicates fitting based on the functions in the text.

YbB_{12} and the temperature difference between the samples was only 6 K. We can also see the effect of the time window here. This effect shows in the form of the following two appearances in the SR-based Mössbauer spectrum: a wavy pattern at the sides of the main absorption and a narrowing effect on the apparent absorption width. For the narrowing effect, when we evaluate the full width at half maximum (FWHM) of this spectrum, via a simple Lorentzian, as a conventional RI Mössbauer spectrum, the FWHM is $1.3 \pm 0.2 \text{ mm/s}$. Because the narrowest ideal width in conventional RI Mössbauer spectroscopy is twice the energy width of the nuclear excited level and is 2.0 mm at FWHM for the 76.5 keV level of ^{174}Yb , the apparent width from this evaluation is narrower than the conventional ideal width. In some cases, this narrowing effect is useful for experimental determination of energy shifts in Mössbauer spectroscopy; e.g., the difference in isomer shifts between Yb^{2+} and Yb^{3+} is considered to be less than 0.2 mm/s in the ^{174}Yb spectrum,⁷ and the line width is therefore critical. We can also narrow the line width by observing a later time window, at the cost of the counting rate.

Further improvements in the counting rate of NRS of SR can be achieved by reducing obstacles to the emitted electrons. Removal of boron nitride from the scatterer enhances the rate because IC electrons cannot travel more than $40 \mu\text{m}$ in boron nitride. The use of a sheet made from single-crystal YbB_{12} satisfies this requirement. Additionally, ^{174}Yb enrichment of the scatterer is effective because Yb nuclides other than ^{174}Yb act as obstacles to electrons and X-rays. The improved time response of the APD detector also enlarges the time window and consequently enhances the counting rate. This is made possible by using smaller area APD elements. Following these improvements, a ten-fold counting rate improvement can be achieved. In the near future, with this enhanced counting rate combined with the SR features, ^{174}Yb SR-based Mössbauer spectroscopy under extreme conditions, e.g., under high pressure in pressure cells or on thin film surfaces, will be realized and will contribute to the study of magnetic phenomena in Yb compounds.

The detection system developed here can also be applied to SR-based Mössbauer spectroscopy with other nuclides. For example, it enables us to perform SR-based Mössbauer spectroscopy using ^{170}Yb . The isomer shift of ^{170}Yb reflects the Yb valence with 2.5 times more sensitivity than that of ^{174}Yb ,⁷ and the valence state is expected to be determined more precisely using the width-narrowing effect in this system. SR-based Mössbauer spectroscopy using ^{171}Yb , ^{172}Yb , and ^{176}Yb is also promising because NRS of SR by these nuclides has also been observed.¹¹ Their IC coefficients are higher than 7, as shown in Table I, and thus the detection system counting IC electrons is efficient for SR-based Mössbauer spectroscopy using these nuclides. This multi-nuclide selectivity will be useful when studying artificially designed devices that contain Yb. For example, we can study Yb-containing interface monolayers sandwiched between other Yb compounds using this multi-nuclide selectivity.¹⁵ Many rare earth nuclides also have high IC coefficients, as shown in Table I, and thus SR-based Mössbauer spectroscopy using these nuclides is also promising for this system.

TABLE I. Promising rare earth nuclides for SR-based Mössbauer spectroscopy.

Nuclides	Energy (keV) ^a	Half-life (ns) ^a	Internal conversion coefficient ^b	Nuclides	Energy (keV) ^a	Half-life (ns) ^a	Internal conversion coefficient ^b
¹⁴⁵ Nd	67.22	29.4	9.61	¹⁶⁴ Dy	73.992	2.39	9.0
¹⁴⁹ Sm	22.507	7.12	29.2	¹⁶⁴ Er	91.40	1.47	4.2
¹⁵⁴ Sm	81.976	3.02	4.94	¹⁶⁶ Er	80.577	1.82	6.88
¹⁵¹ Eu	21.532	9.6	28.0	¹⁶⁸ Er	79.804	1.88	7.14
¹⁵⁵ Gd	86.5460	6.54	9.36	¹⁷⁰ Er	78.68	1.89	7.59
¹⁵⁶ Gd	88.9666	2.21	3.93	¹⁶⁹ Tm	8.4103	4.08	285.0
¹⁵⁷ Gd	63.917	4.6 × 10 ²	0.971	¹⁷⁰ Yb	84.2551	1.60	6.37
¹⁵⁸ Gd	79.510	2.52	6.02	¹⁷¹ Yb	75.878	1.64	9.73
¹⁶⁰ Gd	75.26	2.69	7.44	¹⁷² Yb	78.7436	1.65	8.4
¹⁶⁰ Dy	86.7882	2.02	4.69	¹⁷⁴ Yb	76.471	1.79	9.43
¹⁶¹ Dy	25.65150	29.1	2.35	¹⁷⁶ Yb	82.13	1.76	7.06
¹⁶² Dy	80.660	2.20	6.22				

^aFrom Ref. 23.^bFrom Ref. 24.

Our system also has the potential to dramatically enhance the counting rate of the nuclear resonant inelastic scattering (NRIS) of SR. NRIS is usually used to obtain the phonon density of states (PDOS) of selected nuclides.¹⁶ This selectivity allows determination of the vibrational amplitudes and frequencies of specific atoms with no selection rules, even in complex biological samples. This has provided the opportunity to study structures of reactive intermediates in the catalytic cycles of non-heme iron enzymes via the PDOS of ⁵⁷Fe.^{17–19} The high SR brilliance enables us to measure small samples, and therefore measurements can be performed under extreme conditions in which the accessible sample space is severely limited. Measurements of the PDOS under high pressure with a diamond anvil cell have been performed to study the earth's core.^{20,21} However, NRIS is usually much less intense than nuclear resonant elastic scattering. The high detection efficiency of the system, achieved by the detection of IC electrons and the proximity of the detector to the sample, will compensate for this low intensity. Therefore, our system will bring further improvements to NRIS measurements for small samples and/or samples with dilute resonant nuclides, such as protein single crystals or natural enzymes without enrichment of the resonant nuclides. Additionally, the high detection efficiency can compensate for the low intensity caused by the low reflectivity of the high resolution monochromator used in NRIS experiments. Actually, the bandwidth of a high resolution monochromator is limited above approximately 1 meV because the reflectivity decreases as the reflection with higher Miller index is used to achieve higher resolution. Therefore, if sufficient counting rates can be obtained by using the developed system, the higher resolution monochromator can be used and it provides detailed information on the PDOS from the NRIS experiments. It may also be used to study certain phenomena that are essentially different from PDOS, e.g., boson peaks in glassy materials, because the energy resolution of an ultra-high resolution monochromator can reach 120 μeV.²²

In summary, the IC electron detection system developed here dramatically enhanced the counting rate in SR-based Mössbauer spectroscopy and therefore enables the efficient

measurement. ¹⁷⁴Yb Mössbauer spectroscopy was performed as a feasibility study for this system, and a fivefold increase in the counting rate of NRS of SR by ¹⁷⁴Yb was achieved, while the spectrum of YbB₁₂ was measured without ¹⁷⁴Yb enrichment within 10 h. ¹⁷⁴Yb has the largest natural abundance of Yb nuclides at 31.8%, and we do not need to prepare specially enriched samples for Yb Mössbauer spectroscopy. Since the Mössbauer spectrum in the energy-domain is familiar to many researchers, the efficient measurement achieved using the developed system will offer the benefits a wide variety of scientific areas. Other promising improvements in the counting rate will enable us to realize Mössbauer studies of Yb compounds under extreme conditions, such as high pressure. This system can also be applied efficiently to Mössbauer spectroscopy with many other nuclides and to NRIS experiments.

The authors would like to thank Professor Kishimoto for all his valuable advice during the development of the X-ray windowless detector system. We would also like to thank the Accelerator Group of SPring-8 for their support, especially with the top-up injection operation. These experiments were performed at the BL09XU and BL11XU beamlines of SPring-8 with the approval of the Japan Synchrotron Radiation Research Institute (JASRI) (Power User Priority Program Nos. 2012A0086 and 2013A0086 for BL09XU, and Proposal Nos. 2011B3501 and 2012A3501 for BL11XU). This work was supported by JSPS KAKENHI Grant-in-Aid for Scientific Research (S) of Grant No. 24221005 and Grant-in-Aid for Research Activity Start-up of Grant No. 24810014.

¹J. B. Hastings, D. P. Siddons, U. van Bürck, R. Hollatz, and U. Bergmann, *Phys. Rev. Lett.* **66**, 770 (1991).²I. Sergueev, A. I. Chumakov, T. H. D. Beaume-Dang, R. Rüffer, C. Strohm, and U. van Bürck, *Phys. Rev. Lett.* **99**, 097601 (2007).³S. Kishimoto, F. Nishikido, R. Haruki, K. Shibuya, and M. Koshimizu, *Hyperfine Interact.* **204**, 101 (2012).⁴M. Seto, R. Masuda, S. Higashitaniguchi, S. Kitao, Y. Kobayashi, C. Inaba, T. Mitsui, and Y. Yoda, *Phys. Rev. Lett.* **102**, 217602 (2009).⁵For ⁵⁷Fe Mössbauer spectroscopy using synchrotron radiation, synchrotron radiation source is excellent for energy-domain measurement. See the following articles: A. I. Chumakov, M. V. Zelepukhin, G. V. Smirnov,

- U. van Brück, R. Rüffer, R. Hollatz, H. D. Rüter, and E. Gerdau, *Phys. Rev. B* **41**, 9545 (1990); T. Mitsui, M. Seto, S. Kikuta, N. Hirao, Y. Ohishi, H. Takei, Y. Kobayashi, S. Kitao, S. Higashitaniguchi, and R. Masuda, *Jpn. J. Appl. Phys.* **46**, 821 (2007).
- ⁶For a systematic database, see a textbook of Mössbauer spectroscopy. For example, P. Gütlich, E. Bill, and A. X. Trautwein, *Mössbauer Spectroscopy and Transition Metal Chemistry* (Springer, Berlin, 2011).
- ⁷G. K. Shenoy and F. E. Wagner, *Mössbauer Isomer Shifts* (North-Holland, Amsterdam, 1978), p. 711.
- ⁸E. Kankeleit, *Z. Phys.* **164**, 442 (1961).
- ⁹S. Kishimoto, Y. Yoda, M. Seto, Y. Kobayashi, S. Kitao, R. Haruki, T. Kawauchi, K. Fukutani, and T. Okano, *Phys. Rev. Lett.* **85**, 1831 (2000).
- ¹⁰D. Weschenfelder, H. Schmidt, V. Oestreich, and G. Czjzek, *Hyperfine Interact.* **16**, 1033 (1983).
- ¹¹R. Masuda, S. Higashitaniguchi, S. Kitao, Y. Kobayashi, M. Seto, T. Mitsui, Y. Yoda, R. Haruki, and S. Kishimoto, *J. Phys. Soc. Jpn.* **75**, 094716 (2006).
- ¹²F. Iga, N. Shimizu, and T. Takabatake, *J. Magn. Magn. Mater.* **177–181**, 337 (1998).
- ¹³The internal conversion coefficient to subshells can be calculated based on the following article: T. Kibédi, T. W. Burrows, M. B. Trzhaskovskaya, P. M. Davidson, and C. W. Nestor, Jr., *Nucl. Instrum. Methods Phys. Res. Sect. A* **589**, 202 (2008). This calculation can be performed at <http://bricc.anu.edu.au/>.
- ¹⁴M. Seto, R. Masuda, S. Higashitaniguchi, S. Kitao, Y. Kobayashi, C. Inaba, T. Mitsui, and Y. Yoda, *J. Phys. Conf. Ser.* **217**, 012002 (2010).
- ¹⁵SR-based Mössbauer study of the interface in thin film has been performed using ⁵⁷Fe. For example, see the following: K. Mibu, M. Seto, T. Mitsui, Y. Yoda, R. Masuda, S. Kitao, Y. Kobayashi, E. Suharyadi, M. Tanaka, M. Tsunoda, H. Yanagihara, and E. Kita, *Hyperfine Interact.* **217**, 127 (2013).
- ¹⁶M. Seto, Y. Yoda, S. Kikuta, X. W. Zhang, and M. Ando, *Phys. Rev. Lett.* **74**, 3828 (1995).
- ¹⁷K. Park, T. Tsugawa, H. Furutachi, Y. Kwak, L. V. Liu, S. D. Wong, Y. Yoda, Y. Kobayashi, M. Saito, M. Kurokuzu, M. Seto, M. Suzuki, and E. I. Solomon, *Angew. Chem. Int. Ed.* **52**, 1294 (2013).
- ¹⁸K. Park, C. B. Bell, L. V. Liu, D. Wang, G. Xue, Y. Kwak, S. D. Wong, K. M. Light, J. Zhao, E. E. Alp, Y. Yoda, M. Saito, Y. Kobayashi, T. Ohta, M. Seto, L. Que, and E. I. Solomon, *Proc. Natl. Acad. Sci. U.S.A.* **110**, 6275 (2013).
- ¹⁹S. D. Wong, M. Srncic, M. L. Matthews, L. V. Liu, Y. Kwak, K. Park, C. B. Bell III, E. E. Alp, J. Zhao, Y. Yoda, S. Kitao, M. Seto, C. Krebs, J. M. Bollinger, and E. I. Solomon, *Nature* **499**, 320 (2013).
- ²⁰R. Lübbbers, H. F. Grünsteudel, A. I. Chumakov, and G. Wortmann, *Science* **287**, 1250 (2000).
- ²¹H. K. Mao, J. Xu, V. V. Struzhkin, J. Shu, R. J. Hemley, W. Struhahn, M. Y. Hu, E. E. Alp, L. Vocadlo, D. Alfé, G. D. Price, M. J. Gillan, M. Schwoerer-Böhning, D. Häusermann, P. Eng, G. Shen, H. Giefers, R. Lübbbers, and G. Wortmann, *Science* **292**, 914 (2001).
- ²²M. Yabashi, K. Tamasaku, S. Kikuta, and T. Ishikawa, *Rev. Sci. Instrum.* **72**, 4080 (2001).
- ²³R. B. Firestone and V. S. Shirley, *Table of Isotopes*, 8th ed. (John Wiley & Sons, New York, 1998).
- ²⁴R. Röhlberger, *Nuclear Condensed Matter Physics with Synchrotron Radiation* (Springer-Verlag, Berlin, 2004), p. 303.